

Ectopic chondrogenesis of nude mouse induced by nano gene delivery enhanced tissue engineering technology

This article was published in the following Dove Press journal:
International Journal of Nanomedicine

Guangcheng Zhang¹
Mingjun Nie²
Thomas J Webster³
Qing Zhang²
Weimin Fan¹

¹Department of Orthopedics, the First Affiliated Hospital of Nanjing Medical University, Nanjing, People's Republic of China; ²Department of Orthopedics, Affiliated Hospital of Jiangsu University, Zhenjiang, People's Republic of China; ³Department of Chemical Engineering, Northeastern University, Boston, MA 02115, USA

Background: Many techniques and methods have been used clinically to relieve pain from cartilage repair, but the long-term effect is still unsatisfactory.

Purpose: The objective of this study was to form an artificial chondroid tissue gene enhanced tissue engineering system to repair cartilage defects via nanosized liposomes.

Methods: Cationic nanosized liposomes were prepared and characterized using transmission electron microscope (TEM) and dynamic laser light scattering (DLS). The rat mesenchymal stem cells (rMSCs) were isolated, cultivated, and induced by SRY (Sex-Determining Region Y)-Box 9 (Sox9) via cationic nanosized liposomes. The induced rMSCs were mixed with a thermo-sensitive chitosan hydrogel and subcutaneously injected into the nude mice. Finally, the newly-formed chondroid tissue obtained in the injection parts, and the transparent parts were detected by HE, collagen II, and safranin O.

Results: It was found that the presently prepared cationic nanosized liposomes had the diameter of 85.76 ± 3.48 nm and the zeta potential of 15.76 ± 2.1 mV. The isolated rMSCs proliferation was fibroblast-like, with a cultivated confluence of 90% confluence in 5–8 days, and stained positive for CD29 and CD44 while negative for CD34 and CD45. After transfection with cationic nanosized liposomes, we observed changes of cellular morphology and a higher expression of SOX9 compared with control groups, which indicated that rMSCs could differentiate into chondrocyte in vitro. By mixing transfected rMSCs with the thermo-sensitive hydrogel of chitosan in nude mice, chondroid tissue was successfully obtained, demonstrating that rMSCs can differentiate into chondrogenic cells in vivo.

Conclusion: This study explored new ways to improve the quality of tissue engineered cartilage, thus accelerating clinical transformation and reducing patient pain.

Keywords: Sox9, chondrogenesis, gene enhanced tissue engineering, transfection, chondroid

Introduction

Cartilage injury, a common clinical problem, can be caused by trauma,¹ osteoarthritis,² rheumatoid arthritis,³ and exfoliative chondritis.⁴ Articular cartilage is a non-vascular tissue, whose regeneration ability is extremely limited.^{5,6} Most believe that the damage of mature articular cartilage is partial or superficial, and cartilage cannot regenerate itself.^{7–12} When the lesion is associated with the opening of the subchondral bone, cartilage repair can be completed because of the cells derived from bone marrow and blood vessels of subchondral bone.^{13–15} Even so, the repair cartilage has not been found to be the same as normal cartilage structure and mechanical properties, except embryonic stem cells.^{16,17} To date, no satisfactory method resulted in damaged cartilage

Correspondence: Weimin Fan
Department of Orthopedics, The First Affiliated Hospital of Nanjing Medical University, Nanjing 210029, People's Republic of China
Tel +86 0258 371 4511
Email fanweimin@vip.sina.com

repairing clinically, except when using autologous or xenogenous engrafting.^{18,19} While autologous cartilage presents as feasible to graft, it is hard to obtain adequate matches.^{20–22} Furthermore, all these techniques are subject to the donor site availability.^{23,24} Obtaining hyaline cartilage bio-tissue is a pivotal and serious way for cartilage repair in clinical therapy.

As a natural polysaccharide polymer, chitosan has a homogeneous structure with glucosamine, which is one of the main components of the cartilage matrix, and is increasingly used in cartilage tissue engineering research.^{25,26} For the hydrogel to carry seeded, chitosan has been receiving even more attention.^{27,28} The chitosan hydrogel can be prepared via the interaction of ions or glutaraldehyde crosslinking,²⁹ and its azide derivatives could also be cross-linked under UV irradiation to fabricate hydrogel.^{30–34} Therein, ions are often reacted in hydrogels.

Thermo-sensitive hydrogels made of chitosan own several attractive properties, including mild preparation conditions, a phase transition temperature and body temperature closed to or even lower than the body's temperature, and good biocompatibility and biodegradability.^{35–37} Thus, chitosan has great application potential for tissue engineering and drug controlled-release carrier applications. Based on the physical and chemical as well as biological properties, chitosan can satisfy cell growth, proliferation, and differentiation, to be used as an injectable tissue engineering scaffold material.^{38–40}

Tissue engineering technology, which can grow a mature tissue in vitro, is now extensively used in medicine.^{41,42} A cartilage defect area repaired with tissue engineering technology has achieved a certain effect in vivo and promotes cartilage growth.^{43,44} Meanwhile, engineered repair can provide the appropriate growth space for repair cells, quickly fill the cartilage defect area, prevent unwanted fiber tissue growth,⁴⁵ and provide certain biomechanical support for the early repair.^{46,47} Chondrocytes and bone marrow stromal stem cells are commonly used to construct the cartilage.

However, tissue engineering technology also has its limitations, such as limited cell sources, and it is easy to cause the defects on such materials. In contrast, gene-enhanced tissue engineering technology has significantly more hope for cartilage repair.^{48,49} To solve these problems, this study explored a new therapeutic approach for the treatment of cartilage defects using bone marrow stromal stem cells. Compared to the viral vectors, non-viral systems have attracted significant

attention to the cost-effectiveness and less induction of the immune system in gene delivery. A lot of nano non-viral gene vectors have been reported, which include polymer (PAMAM,^{50,51} PEI⁵²), protein,⁵³ liposomes,^{54,55} and so on, due to their low toxicity, antigenicity, high entrapment efficiency, and good stability.^{56,57}

The Sox gene family is a newly-discovered gene family whose main feature is a conservative base sequence HMG-box, which can be combined with DNA sequence specificity.⁵⁸ The gene family plays an important role in embryonic development, gender differentiation, nervous system, repair, and skeletal system development. Sox9 protein is considered to have an important effect on skeletal system development.⁵⁹ Animal experiments showed that the Sox9 had a high expression, and control of type II collagen synthesis in both embryonic cartilage germinal parts, thus, strongly infecting the formation of cartilage.

Liposomes have been well established as an effective drug delivery system, due to their preparation simplicity and unique characteristics.⁶⁰ In this article, we fabricated cationic liposomes of uniform morphology. Then, rat bone marrow stromal stem cells (rMSCs) were cultivated and proliferated in vitro. The rMSCs were transfected with Sox9 gene via cationic liposomes, combined with thermal-sensitive injectable chitosan composite scaffolds for tissue engineering cartilage in vitro and implanted into nude mice to build chondroid tissue.

Materials and methods

Materials

All experimental protocols were approved by the First Affiliated Hospital of Nanjing Medical University and followed the principles of laboratory and animal care of the university. (2,3-Dioleoyloxy-propyl)-trimethylammonium (DOTAP) and 1,2-dioleoyl-sn-glycero-3-phosphocholine (DOPC) were purchased from A.V.T. (Shanghai) Pharmaceutical Co., Ltd. Hoechst 33342 and 3-[4, 5-dimethylthiazol-2-yl]-2, 5-diphenyltetrazolium bromide (MTT) were purchased from Sigma-Aldrich (Cambridge, MA, USA). Sox9 plasmid was purchased from Bioworld Technology, Inc., China (PPL00081-2b) a, and the species of the Sox9 plasmid is *Homo sapiens* (human) with vector backbone of pcDNA3 (Figure S1). Dulbecco's modified Eagle's medium (DMEM) and fetal bovine serum (FBS) were bought from Gibco BRL (Thermo Fisher, USA). Additionally, Penicillin-streptomycin, 0.25% trypsin-EDTA, and non-essential amino acid were obtained from

Invitrogen (Thermo Fisher), anti-Collagen II (ab34712) and anti-collagen IX (ab134568) were bought from Abcam (USA), Streptavidin-Biotin Complex (SABC) kit was purchased from Boster (SA1025, USA). Other chemicals used in this work were all of the analytical pure grades and were used as received.

The fabrication and characterization of cationic liposomes

The thin membrane method was employed to prepare cationic liposomes.^{61,62} Briefly, DOTAP (350 mg) was dissolved in chloroform (1 mL) and mixed with DOPC of 370 mg. The mixture was diluted to 1.0 mL in total using chloroform and vortexed for 10 minutes. The solvent was evaporated in rotary evaporator (Buchi R) at 50°C, and a thin film of dry lipid on the flask was obtained. Evaporation was continued for 1 hour after drying to remove the residue solvent. The lipid film was ground into a powder and dissolved in 4 mL water under vigorous stirring to form cationic liposomes. The formulation was further characterized by transmission electron microscopy (TEM, JEOL) and dynamic laser scattering (DLS, Malvern). The results were represented by the averages of six measurements per sample with 20 seconds spent on each measurement. All measurements were performed at 25°C.

The separation, culture, and generation of MSCs in rats

Rat bone marrow was extracted from the 5–6 weeks old Sprague Dawley (SD) rat hind legs, diluted with D-Hanks for thorough incorporation, and centrifuged at 800 rpm for 5 minutes. The supernatant was abandoned, and DMEM was used to gently scatter cells into single cells suspension. The suspension was slowly added to lymphocyte density separation medium ($\rho=1.077 \text{ g cm}^{-3}$) and centrifuged at 3,000 rpm for 20 minutes. The mononuclear cell layer was taken and washed by D-Hanks twice, and DMEM containing 20% FBS was added to the cells in the flask for further cultivation. A growth curve of rMSCs was detected by a trypan blue experiment. The flask was incubated at 37°C and 5% CO₂ in the incubator. The medium was replaced after 48 hours, and the unattached cells were abandoned. The cells were observed daily under an inverted phase contrast microscope. After being confluent, the cells were digested with trypsin and passaged. The third generation was identified by flow cytometry with CD34, CD45, CD29, and CD44.

The liposomes mediate Sox9 gene transfection with targeted chondrogenic differentiation

The transfection followed previous reports,⁶³ where briefly the recombinant Sox9 plasmid was diluted and mixed with cationic liposomes without FBS for 20 minutes at room temperature. The mixture was added directly to rMSCs in a petri dish and cultivated at 37°C, 95% humidity, and 5% CO₂ training. The medium was replaced with the full medium after 4 hours and continued to develop after 36 hours to detect the transfection efficiency. Cell transfection was divided into three groups: 1) the experimental group: cationic liposomes were used to carry out the recombinant plasmid transfection of Sox9; 2) the control group: transfection of empty plasmid; 3) a blank control group: only the equivalent cationic liposomes were added; and 4) Lipofectamine 2000 was used as a positive control for the Sox9 plasmid transfection. After 7 days of culture, ELISA was used to characterize the tissue engineering materials cultured in the cells. At the 7 days transfection, confluence at 80~90% of the third generation of rMSCs was taken and Sox9 determined by ELISA for five parallel specimens from each sample. To optimize the transfection of cationic nanosized liposomes, a serial concentration of DNA plasmid (10, 50, 100, 200 ng) was used to transfect in different cell numbers for transfection (1×10^4 , 2×10^4 , 4×10^4 , 8×10^4 cells per well). The transfected cells were collected, and the protein was extracted to detect the Sox9 protein expression via ELISA. Statistical analysis was performed on the computer, with SPSS statistical software. $\bar{X} \pm S$ was used to indicate that $P=0.05$.

Preparation of thermos-sensitive chitosan gel

A thermo-sensitive gel was prepared as previously described.⁶⁴ Briefly, chitosan was added into 0.1 mol L^{-1} hydrochloric acid solution to make the final concentration 2% (w/v), which formed solution A. β -sodium glycerophosphate were prepared in water at 56% (w/v), which formed solution B. Then two solutions were combined and mixed at different ratios (v/v) to form a thermosensitive hydrogel. The various ratios of the prepared hydrogels were kept at 4°C and tested at 37°C for temperature sensitive properties.

Chondrogenesis in vivo

The rMSCs were transfected and cultivated for 2 weeks, blended with thermo-sensitive chitosan hydrogel (0.2 mL), and subcutaneously injected into the back of nude mice. The

in vivo experiments with nude mice were divided into two groups: untransfected rMSCs with chitosan hydrogel (group A) and transfected rMSCs with chitosan hydrogel (group B). After 4 weeks of feeding, the subcutaneous injections were observed for the formation of cartilage in nude mice, including hematoxylin-eosin (HE) and safranin O staining. The immunohistochemistry (IHC) of collagen II and collagen IX of different groups were stained and labeled with SABC kit. Western blot (WB) of Sox9, collagen II and collagen IX were processed to quantify the chondrogenic of different groups.

Statistical analysis

Data of each group is represented by $\bar{X} \pm s$. SPSS Statistical software was used for statistical analysis. One-way ANOVA was used for multi-group data. A two sample *t*-test was used between the two groups of data. $P < 0.05$ and $P < 0.01$ were statistically significant.

Results

Characterization of cationic liposomes

The mean particle size of the cationic liposomes was 85.76 ± 3.48 nm (Figure 1A) with a PDI value of 0.22 and a zeta potential of 15.76 ± 2.1 mV (Figure 1B), which indicated the monodispersed nature of the nanoparticles. TEM of cationic liposomes had the same results as that of DLS, with an expected small size less than 100 nm with nearly spherical and uniform shape (Figure 1C).

Cells morphological observation of rMSCs

After inoculation, rMSCs were distributed at the bottom of the culture flask, and they were round with a bright cytoplasm and good refraction. The individual nucleus in the cells

began to adhere to the wall (Figure 2A, 24 h) at 24 hours; increased spreading and the cytoplasm extending outward, similar to fibroblasts (Figure 2A, 48 h) at 48 hours, and the morphology of the adherent cells was fusiform, triangular, fan-shaped, and circular, and, after 5–8 days, the cells gradually formed a scattered colony, which is called a fibroblast colony (Figure 2A, 5–8 d). Flow cytometry was used to observe the expression of CD29 (95.34%) and D44 (85.12%), while CD34 (4.69%) and CD45 (5.12%) were negative (Figure 2B). A cell proliferation growth curve was drawn according to the determination by MTT (Figure 2C).

Cells morphological observation of chondrogenic differentiation of rMSCs after gene transfection

After rMSCs were transfected with Sox9 for 7 days, cells protrusion became longer, the body of the cell became wider, and the refractive index increased (Figure 3A). The growth curve is shown using the MTT method, and the proliferation rate of transfected cells increased (Figure 3B). The expression of Sox9 of rMSCs was detected by ELISA at different concentrations of cells (Figure 3C), which showed that the level of Sox9 expression in the experimental group was significantly higher than the other groups ($P < 0.05$, Figure 3D).

Thermosensitive gel preparation

The various chitosan hydrogels kept at 4°C were incubated at 37°C for 1–5 minutes to observe the hydrogel formation process. Compared with the different gelation times of the ratio of chitosan and β -sodium glycerophosphate, we found that the gelation time⁶⁵ rapidly decreased from 15 minutes to 3 minutes with an increase of β -sodium glycerophosphate (Table 1).

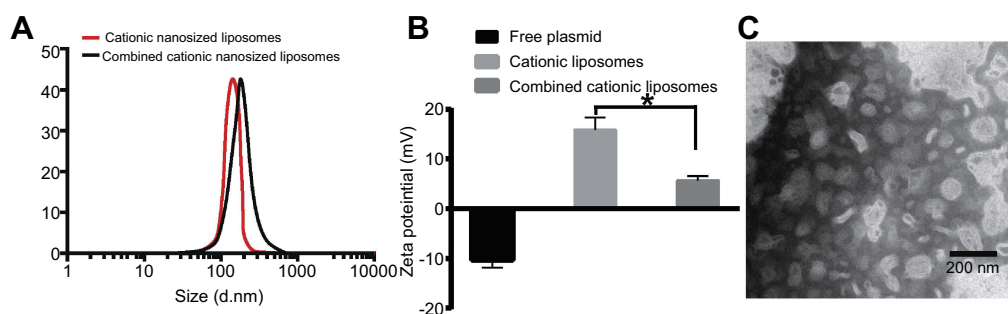


Figure 1 Characterization of cationic liposomes. (A) The diameter of cationic liposomes, (B) The zeta potential of cationic liposomes, and (C) TEM of cationic liposomes. * $P < 0.01$.

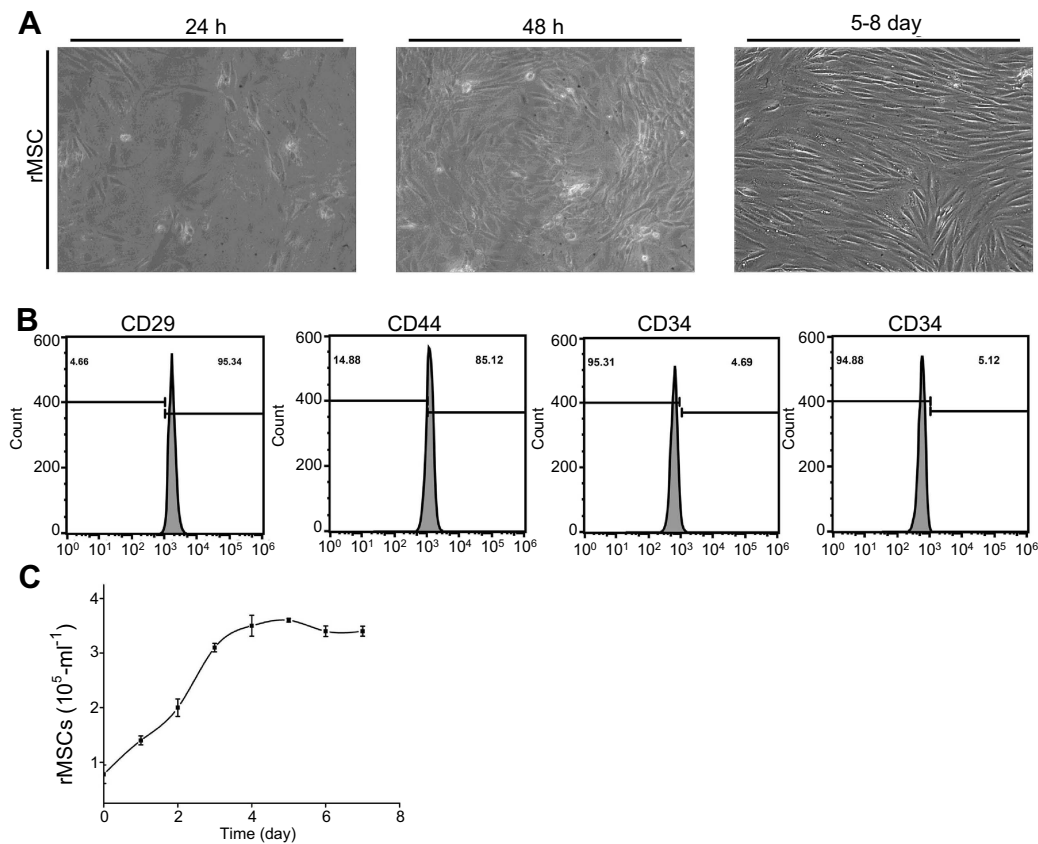


Figure 2 Isolated rMSCs cultivation and identification. (A) Isolated rMSCs cultivated at different times (24 hours, 48 hours, 5–8 day); (B) identification of rMSCs by flow cytometry; (C) growth curve of rMSCs.

Chondrogenesis in vivo

The transfected rMSCs and thermos-sensitive gel compound were cultured and injected into nude mice to observe chondrogenesis (Figure 4). The nude mice were sacrificed, and injection areas were anatomized after feeding for 4 weeks. We only found mass like structures in group A (untransfected rMSCs with chitosan hydrogel) and group B (transfected rMSCs with chitosan hydrogel), while no structures in group C (rMSCs) and group D (chitosan hydrogel) were observed. The mass like structures in group A and B were examined by HE, safranin O, and immunohistochemical staining of collagen II. Compared to group A, the formation of chondroid cells at the surface of tissue was observed, and the cytoplasm was brown after being dewaxed, while the nucleus was vacuolar in group B. HE staining of tissue-engineered cartilage blocks showed the aggregation of cells at the surface tissue, similar to chondrocyte expression (Figure 5). The results of immunohistochemical stain of collagen II and IX showed the significant difference between two groups. Furthermore, the WB of different groups

illustrated the different protein expression of Sox9, collagen II, and collagen IX.

Discussion

The nude mice were injected with induced rMSCs and chitosan hydrogel, with the chitosan hydrogel alone disappearing under the skin while chondrocyte formation was found (Figure 4). In recent years, many have shown that rMSCs are the best choice for the seed cells of cartilage tissue engineering,^{66–69} but the amount of rMSCs is extremely low for this purpose, limiting its application in tissue engineering. Proliferation rMSCs in vitro has been examined and potentially developed,⁷⁰ leading to mature protocols for isolation culture and amplification. In order to improve the quality of tissue engineering cartilage, it has become necessary to induce the differentiation of the seed cells into the chondrocytes before inserting the seed cells into the carrier materials. For the application of cells in tissue engineering technology in our study, we prepared cationic liposomes, extracted the bone marrow tissue from

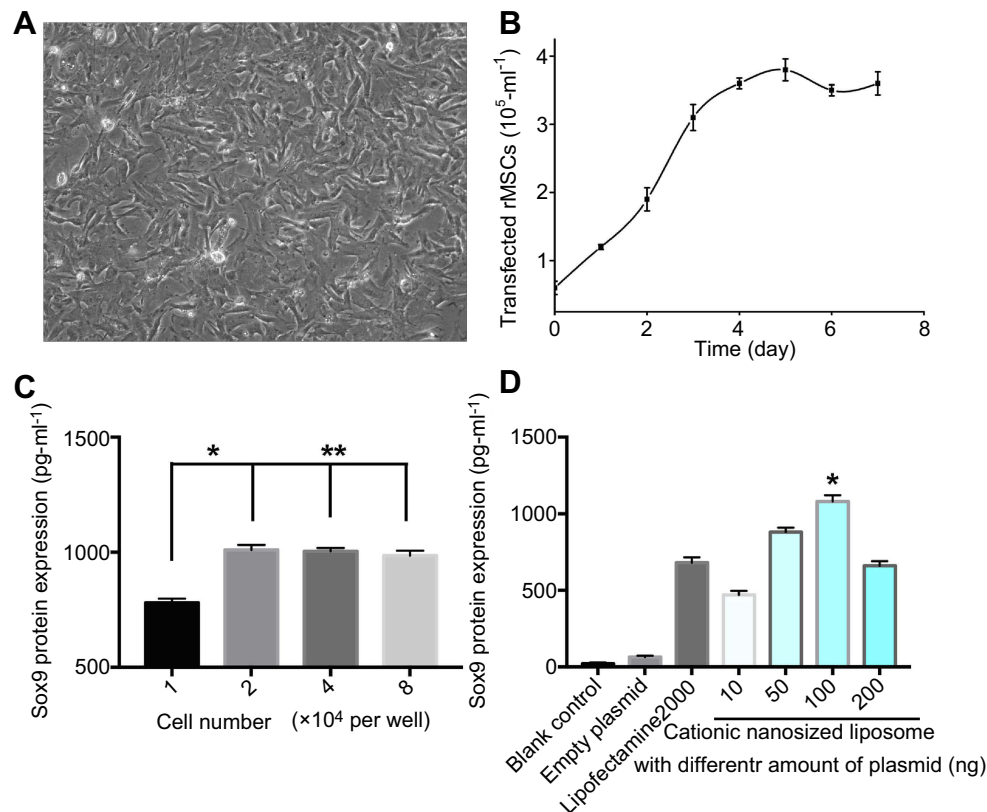


Figure 3 In vitro transfection of rMSCs. (A) rMSCs were transfected for 7 days; (B) growth curve of transfected rMSCs; (C) gene transfection of rMSCs with cationic nanosized liposomes at different concentrations of cells (* $P < 0.05$; ** $P > 0.05$). (D) Gene transfection of rMSCs with different formulations.

Table 1 Different ratio of chitosan and β -glycerophosphate on GT

Chitosan (2%): β -glycerophosphate (50%) (V:V)	GT (minutes)
5	3
7	15
10	50

Abbreviation: GT, gelation time.

rats, isolated rMSCs, increased rMSCs culture cell number in vitro, and transfected them with Sox9 to differentiate into cartilage producing cells. The results showed that

rMSCs were able to maintain the stem cell characteristics after proliferation and differentiation in vitro (Figure 2). The fusogenic property of DOPC plays a crucial role in macropinocytic transfer of formulation through the bilayer, resulting in enhanced cellular uptake.^{71,72} However, it remains to be explored whether a specific phenotype of rMSCs can be expressed after long periods after such proliferation and permanent biochemical and directional differentiation.

Although rMSCs studies demonstrate the prospect of new cartilage repair, rMSCs should be combined with

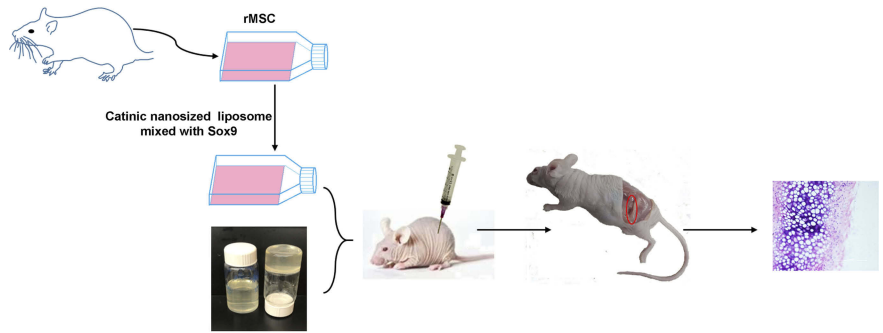


Figure 4 Sketch of Sox9 gene enhanced tissue engineering in chondrogenesis.

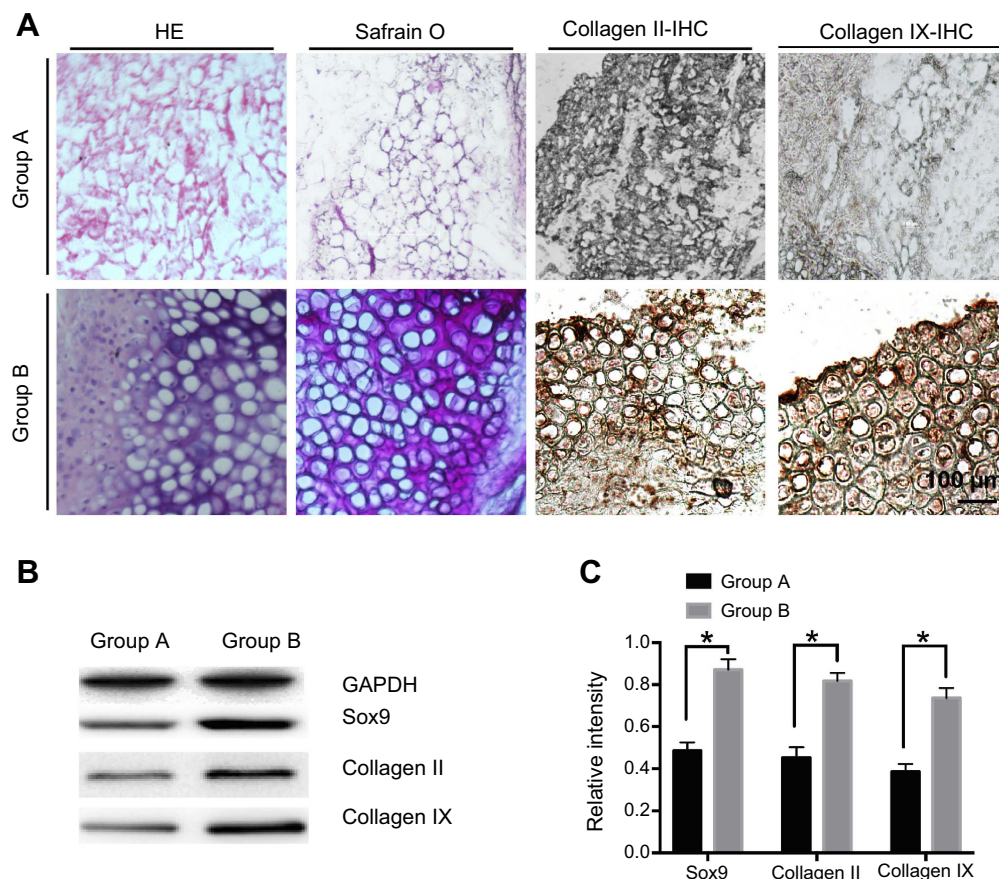


Figure 5 In vivo chondrogenesis of rMSCs. **(A)** Immunohistochemical stain of different groups. **(B)** Western blot (WB) analysis of Sox9, collagen II, and collagen IX. **(C)** Densitometric analysis of Sox9, collagen II, and collagen IX. Group A, untransfected rMSCs with chitosan hydrogel; Group B, transfected rMSCs with chitosan hydrogel. * $P < 0.05$.

recombinant growth factors or organic combination with gene therapy if healing is to be complete. Sox9 has an effect on promoting cell proliferation effect and effectively maintains the phenotype of cartilage cells;^{73–77} it also has to have biological activities at low concentrations. The direct application of Sox9 still has certain limitations, while genetic recombination and transfer technology will be available with the insertion of exogenous genes into eukaryotic cells. The expression of Sox9 can promote bone damage repair and the cartilage cell proliferation. Methods of transfection of eukaryotic cells include cationic liposome membrane fusion, electrophoresis, microinjection, calcium phosphate precipitation, etc. The present cationic liposome method is the most convenient and most commonly used method for transfection, which is suitable for transfection of multiple cells and is the only non-viral vector method approved by the FDA for clinical treatment.^{78–80} In this report, we fabricated nanosized cationic liposomes, and the zeta potential reduced while combined with negative plasmids (Figure 1B). We transfected rMSCs and obtained

the chondroid phenotype. With the liposome transfection technique, the expression of Sox9 was detected with ELISA method (Figure 3C). All the results showed that Sox9 can be stably expressed after induction into the chondroid phenotype from the MSCs. Meanwhile, collagen II was detected by immunocytochemistry stained collagen type II. This indicates that the rMSCs stabilized the expression of Sox9 and induced the chondrogenic phenotype. The immunohistochemical staining of tissue engineering cartilage was observed (Figure 5), and the staining of tissue-engineered cartilage blocks showed the aggregation of cells in the surface tissue, similar to chondrocyte expression in group B. All the results demonstrated that chondroid tissue formed in group B (the transfected rMSCs combined with chitosan hydrogel), which could offer a new hope for cartilage repair.

The contributions of this study are the unique combination of tissue engineering with genetic engineering to develop an effective and convenient therapeutic approach for the repair of cartilage defects. Sox9 gene transfected

with rMSCs selected in this study can continuously secrete Sox9 in rMSCs and avoid the need of Sox9 systemic or direct injection doses which can lead to unwanted side-effects. In addition, the carrier materials selected in this study can be injected with a chitosan gel and high biosafety. Furthermore, we obtained chondroid tissue in the naked mice model showing that the cartilage can be formed instead of a mixture of scaffolds and cells, which could bring a qualitative leap of clinic cartilage repair.

Conclusion

In summary, this study effectually differentiated rMSCs into chondrocytes in vivo for cartilage repair in vivo yields consistently satisfactory results. This method provides a valuable source of large numbers of MSC, which can be used for cartilage repair in vivo, with the role of Sox9 in chondrogenic differentiation via cationic liposomes. The isolation of rMSCs developed here may be useful in future investigations of stem cells for cartilage repair instead of the limited number of chondrocytes available for cartilage repair. Most importantly, this study showed that, compared with untransfected rMSCs, transfected rMSCs mixed with thermo-sensitive hydrogel could significantly increase chondroid tissue synthesis. All in all, the present gene enhanced tissue engineered artificial cartilage via cationic liposomes was successfully formed under the skin of nude mice, which should be further studied for improved clinic cartilage repair.

Author contributions

Guangcheng Zhang and Weimin Fan designed experiments and acquisitioned data, Guangcheng Zhang and Mingjun Nie analyzed data, Guangcheng Zhang drafted the manuscript, Qing Zhang contributed to intellectual content and Weimin Fan contributed to final approval of the version. All authors contributed to data analysis, drafting and revising the article, gave final approval of the version to be published, and agree to be accountable for all aspects of the work.

Disclosure

The authors report no conflicts of interest in this work.

References

- Babichenko IK. [Cartilage injury of the patella, femoral condyles and knee in trauma to the knee joint]. *Ortop Travmatol Protez*. 1970;31:34–39.
- Hofmann FC, Neumann J, Heilmeier U, et al. Conservatively treated knee injury is associated with knee cartilage matrix degeneration measured with MRI-based T2 relaxation times: data from the osteoarthritis initiative. *Skeletal Radiol*. 2018;47:93–106. doi:10.1007/s00256-017-2759-6
- Bao CX, Chen HX, Mou XJ, Zhu XK, Zhao Q, Wang XG. GZMB gene silencing confers protection against synovial tissue hyperplasia and articular cartilage tissue injury in rheumatoid arthritis through the MAPK signaling pathway. *Biomed Pharmacother*. 2018;103:346–354. doi:10.1016/j.biopha.2018.04.023
- Biquet V. [Case of relapsing erythroderma psoriaticum with multiple arthropathies and developing into osteolysis]. *Arch Belg Dermatol Syphiligr*. 1954;10:58–61.
- Ito H, Moritoshi F, Hashimoto M, Tanaka M, Matsuda S. Control of articular synovitis for bone and cartilage regeneration in rheumatoid arthritis. *Inflamm Regen*. 2018;38:7. doi:10.1186/s41232-018-0064-y
- Qi C, Liu J, Jin Y, et al. Photo-crosslinkable, injectable sericin hydrogel as 3D biomimetic extracellular matrix for minimally invasive repairing cartilage. *Biomaterials*. 2018;163:89–104. doi:10.1016/j.biomaterials.2018.02.016
- Filardo G, Perdida F, Gelinsky M, et al. Novel alginate biphasic scaffold for osteochondral regeneration: an in vivo evaluation in rabbit and sheep models. *J Mater Sci Mater Med*. 2018;29:74. doi:10.1007/s10856-018-6074-0
- Mathis DT, Kaelin R, Rasch H, Arnold MP, Hirschmann MT. Good clinical results but moderate osseointegration and defect filling of a cell-free multi-layered nano-composite scaffold for treatment of osteochondral lesions of the knee. *Knee Surg Sports Traumatol Arthroscopy*. 2018;26:1273–1280. doi:10.1007/s00167-017-4638-z
- Fan MP, Si M, Li BJ, et al. Cell therapy of a knee osteoarthritis rat model using precartilaginous stem cells. *Eur Rev Med Pharmacol Sci*. 2018;22:2119–2125. doi:10.26355/eurrev_201804_14745
- Behrou R, Foroughi H, Haghpahan F. Numerical study of temperature effects on the poro-viscoelastic behavior of articular cartilage. *J Mech Behav Biomed Mater*. 2018;78:214–223. doi:10.1016/j.jmbbm.2017.11.023
- Aurich M, Koenig V, Hofmann G. Comminuted intraarticular fractures of the tibial plateau lead to posttraumatic osteoarthritis of the knee: current treatment review. *Asian J Surg*. 2018;41:99–105. doi:10.1016/j.asjsur.2016.11.011
- Lindstrom E, Rizoska B, Tunblad K, et al. The selective cathepsin K inhibitor MIV-711 attenuates joint pathology in experimental animal models of osteoarthritis. *J Transl Med*. 2018;16:56. doi:10.1186/s12967-018-1425-7
- Dias IR, Viegas CA, Carvalho PP. Large animal models for osteochondral regeneration. *Adv Exp Med Biol*. 2018;1059:441–501. doi:10.1007/978-3-319-76735-2_20
- Zhang Y, Zhang J, Chang F, Xu W, Ding J. Repair of full-thickness articular cartilage defect using stem cell-encapsulated thermogel. *Mater Sci Eng C Mater Biol Appl*. 2018;88:79–87. doi:10.1016/j.msec.2018.02.028
- Lamplot JD, Schafer KA, Matava MJ. Treatment of failed articular cartilage reconstructive procedures of the knee: a systematic review. *Orthop J Sports Med*. 2018;6:2325967118761871. doi:10.1177/2325967118761871
- Keller L, Wagner Q, Schwinte P, Benkirane-Jessel N. Double compartmented and hybrid implant outfitted with well-organized 3D stem cells for osteochondral regenerative nanomedicine. *Nanomedicine (Lond)*. 2015;10:2833–2845. doi:10.2217/nnm.15.113
- Diaz-Flores L Jr., Gutierrez R, Madrid JF, et al. Cell sources for cartilage repair; contribution of the mesenchymal perivascular niche. *Front Biosci (Schol Ed)*. 2012;4:1275–1294.
- Stone KR, Pelsis JR, Na K, Walgenbach AW, Turek TJ. Articular cartilage paste graft for severe osteochondral lesions of the knee: a 10- to 23-year follow-up study. *Knee Surg Sports Traumatol Arthrosc*. 2017;25:3824–3833. doi:10.1007/s00167-016-4323-7
- Chun YS, Kim KW, Kim JC. Autologous tragal perichondrium patch graft for ahmed glaucoma valve tube exposure. *J Glaucoma*. 2013;22:e27–e30. doi:10.1097/IJG.0b013e318255dc1c

20. Wong CC, Chen CH, Chan WP, et al. Single-stage cartilage repair using platelet-rich fibrin scaffolds with autologous cartilaginous grafts. *Am J Sports Med.* **2017**;45:3128–3142. doi:10.1177/0363546517719876
21. Cole BJ, Farr J, Winalski CS, et al. Outcomes after a single-stage procedure for cell-based cartilage repair: a prospective clinical safety trial with 2-year follow-up. *Am J Sports Med.* **2011**;39:1170–1179. doi:10.1177/0363546511399382
22. Schagemann JC, Erggelet C, Chung HW, Lahm A, Kurz H, Mrosek EH. Cell-laden and cell-free biopolymer hydrogel for the treatment of osteochondral defects in a sheep model. *Tissue Eng Part A.* **2009**;15:75–82. doi:10.1089/ten.tea.2008.0087
23. Confalonieri D, Schwab A, Walles H, Ehlicke F. Advanced therapy medicinal products: a guide for bone marrow-derived MSC application in bone and cartilage tissue engineering. *Tissue Eng Part B Rev.* **2018**;24:155–169. doi:10.1089/ten.TEB.2017.0305
24. Sinkin JC, Yi S, Wood BC, et al. Upper eyelid coloboma repair using accessory preauricular cartilage in a patient with goldenhar syndrome: technique revisited. *Ophthalmic Plast Reconstr Surg.* **2017**;33:e4–e7. doi:10.1097/IOP.0000000000000360
25. Donati I, Stredanska S, Silvestrini G, et al. The aggregation of pig articular chondrocyte and synthesis of extracellular matrix by a lactose-modified chitosan. *Biomaterials.* **2005**;26:987–998. doi:10.1016/j.biomaterials.2004.04.015
26. Sechrist VF, Miao YJ, Niyibizi C, et al. GAG-augmented polysaccharide hydrogel: a novel biocompatible and biodegradable material to support chondrogenesis. *J Biomed Mater Res.* **2000**;49:534–541.
27. Wang W, Wan Y, Fu T, et al. Effect of cyclic compression on bone marrow mesenchymal stromal cells in tissue engineered cartilage scaffold. *J Biomed Mater Res A.* **2019**. doi:10.1002/jbm.a.36642
28. Yuan D, Chen Z, Xiang X, et al. The establishment and biological assessment of a whole tissue-engineered intervertebral disc with PBST fibers and a chitosan hydrogel in vitro and in vivo. *J Biomed Mater Res B Appl Biomater.* **2019**. doi:10.1002/jbm.b.34323
29. Da Silva L, Todaro V, Do Carmo FA, et al. A promising oral fucoidan-based antithrombotic nanosystem: development, activity and safety. *Nanotechnology.* **2018**. doi:10.1088/1361-6528/aae5b
30. Qiao X, Peng X, Qiao J, et al. Evaluation of a photocrosslinkable hydroxyethyl chitosan hydrogel as a potential drug release system for glaucoma surgery. *J Mater Sci Mater Med.* **2017**;28:149. doi:10.1007/s10856-017-5954-z
31. Buchovec I, Lukseviciute V, Kokstaite R, Labeikyte D, Kaziukonyte L, Luksiene Z. Inactivation of gram (-) bacteria *Salmonella enterica* by chlorophyllin-based photosensitization: mechanism of action and new strategies to enhance the inactivation efficiency. *J Photochem Photobiol B.* **2017**;172:1–10. doi:10.1016/j.jphotobiol.2017.05.008
32. Hattori H, Amano Y, Nogami Y, Kawakami M, Yura H, Ishihara M. Development of a novel emergency hemostatic kit for severe hemorrhage. *Artif Organs.* **2013**;37:475–481. doi:10.1111/aor.12004
33. Masuoka K, Ishihara M, Asazuma T, et al. The interaction of chitosan with fibroblast growth factor-2 and its protection from inactivation. *Biomaterials.* **2005**;26:3277–3284. doi:10.1016/j.biomaterials.2004.07.061
34. Ono K, Saito Y, Yura H, et al. Photocrosslinkable chitosan as a biological adhesive. *J Biomed Mater Res.* **2000**;49:289–295.
35. Tang B, Shan J, Yuan T, et al. Hydroxypropylcellulose enhanced high viscosity endoscopic mucosal dissection intraoperative chitosan thermosensitive hydrogel. *Carbohydr Polym.* **2019**;209:198–206. doi:10.1016/j.carbpol.2018.12.103
36. Morsi NM, Nabil Shamma R, Osama Eladawy N, Abdelkhalek AA. Bioactive injectable triple acting thermosensitive hydrogel enriched with nano-hydroxyapatite for bone regeneration: in-vitro characterization, Saos-2 cell line cell viability and osteogenic markers evaluation. *Drug Dev Ind Pharm.* **2019**;45:1–18.
37. Xu X, Gu Z, Chen X, et al. An injectable and thermosensitive hydrogel: promoting periodontal regeneration by controlled-release of aspirin and erythropoietin. *Acta Biomater.* **2019**;86:235–246. doi:10.1016/j.actbio.2019.01.001
38. Qu Y, Tang J, Liu L, Song L, Chen S, Gao Y. Alpha-Tocopherol liposome loaded chitosan hydrogel to suppress oxidative stress injury in cardiomyocytes. *Int J Biol Macromol.* **2019**;125:1192–1202. doi:10.1016/j.ijbiomac.2018.09.092
39. Qu C, Bao Z, Zhang X, et al. A thermosensitive RGD-modified hydroxybutyl chitosan hydrogel as a 3D scaffold for BMSCs culture on keloid treatment. *Int J Biol Macromol.* **2019**;125:78–86. doi:10.1016/j.ijbiomac.2018.12.058
40. Cheng YH, Ko YC, Chang YF, Huang SH, Liu CJ. Thermosensitive chitosan-gelatin-based hydrogel containing curcumin-loaded nanoparticles and latanoprost as a dual-drug delivery system for glaucoma treatment. *Exp Eye Res.* **2019**;179:179–187. doi:10.1016/j.exer.2018.11.017
41. Grath A, Dai G. Direct cell reprogramming for tissue engineering and regenerative medicine. *J Biol Eng.* **2019**;13:14. doi:10.1186/s13036-019-0144-9
42. Bezhaeva T, Geelhoed WJ, Wang D, et al. Contribution of bone marrow-derived cells to in situ engineered tissue capsules in a rat model of chronic kidney disease. *Biomaterials.* **2019**;194:47–56. doi:10.1016/j.biomaterials.2018.12.014
43. Kalamegam G, Memic A, Budd E, Abbas M, Mobasheri A. A comprehensive review of stem cells for cartilage regeneration in osteoarthritis. *Adv Exp Med Biol.* **2018**;2:23–36.
44. Sarem M, Arya N, Heizmann M, et al. Interplay between stiffness and degradation of architected gelatin hydrogels leads to differential modulation of chondrogenesis in vitro and in vivo. *Acta Biomater.* **2018**;69:83–94. doi:10.1016/j.actbio.2018.01.025
45. Patel JM, Merriam AR, Culp BM, Gatt CJ Jr., Dunn MG. One-year outcomes of total meniscus reconstruction using a novel fiber-reinforced scaffold in an ovine model. *Am J Sports Med.* **2016**;44:898–907. doi:10.1177/0363546515624913
46. Khurshid M, Mulet-Sierra A, Adesida A, Sen A. Osteoarthritic human chondrocytes proliferate in 3D co-culture with mesenchymal stem cells in suspension bioreactors. *J Tissue Eng Regen Med.* **2018**;12:e1418–e1432. doi:10.1002/term.2531
47. Zhou Y, Liang K, Zhao S, et al. Photopolymerized maleilated chitosan/methacrylated silk fibroin micro/nanocomposite hydrogels as potential scaffolds for cartilage tissue engineering. *Int J Biol Macromol.* **2018**;108:383–390. doi:10.1016/j.ijbiomac.2017.12.032
48. Yang X, Lu Z, Wu H, Li W, Zheng L, Zhao J. Collagen-alginate as bioink for three-dimensional (3D) cell printing based cartilage tissue engineering. *Mater Sci Eng C Mater Biol Appl.* **2018**;83:195–201. doi:10.1016/j.msec.2017.09.002
49. Venkatesan JK, Moutos FT, Rey-Rico A, et al. Chondrogenic differentiation processes in human bone marrow aspirates seeded in three-dimensional woven poly(epsilon-caprolactone) scaffolds enhanced by rAAV-mediated SOX9 gene transfer. *Hum Gene Ther.* **2018**. doi:10.1089/hum.2017.165
50. Li J, Liang H, Liu J, Wang Z. Poly (amidoamine) (PAMAM) dendrimer mediated delivery of drug and pDNA/siRNA for cancer therapy. *Int J Pharm.* **2018**;546:215–225. doi:10.1016/j.ijpharm.2018.05.045
51. Kretzmann JA, Evans CW, Norret M, Blancafort P, Swaminathan Iyer K. Non-viral methodology for efficient co-transfection. *Methods Mol Biol.* **2018**;1767:241–254. doi:10.1007/978-1-4939-7774-1_13
52. Jia Y, Niu D, Li Q, et al. Effective gene delivery of shBMP-9 using polyethyleneimine-based core-shell nanoparticles in an animal model of insulin resistance. *Nanoscale.* **2019**;11:2008–2016. doi:10.1039/c8nr08193j
53. Terry TL, Givens BE, Rodgers VGJ, Salem AK. Tunable properties of Poly-DL-lactide-monomethoxypolyethylene glycol porous micro-particles for sustained release of polyethylenimine-DNA polyplexes. *AAPS PharmSciTech.* **2019**;20:23. doi:10.1208/s12249-018-1215-9

54. Mattern-Schain SI, Fisher RK, West PC, et al. Cell mimetic liposomal nanocarriers for tailored delivery of vascular therapeutics. *Chem Phys Lipids*. 2019;218:149–157. doi:10.1016/j.chemphyslip.2018.12.009
55. Hattori Y, Nakamura M, Takeuchi N, et al. Effect of cationic lipid in cationic liposomes on siRNA delivery into the lung by intravenous injection of cationic lipoplex. *J Drug Target*. 2019;27:217–227. doi:10.1080/1061186X.2018.1502775
56. Katz MG, Fargnoli AS, Williams RD, Bridges CR. Gene therapy delivery systems for enhancing viral and nonviral vectors for cardiac diseases: current concepts and future applications. *Hum Gene Ther*. 2013;24:914–927. doi:10.1089/hum.2013.2517
57. Nayerossadat N, Maedeh T, Ali PA. Viral and nonviral delivery systems for gene delivery. *Adv Biomed Res*. 2012;1:27. doi:10.4103/2277-9175.98152
58. Guimont P, Grondin F, Dubois CM. Sox9-dependent transcriptional regulation of the proprotein convertase furin. *Am J Physiol Cell Physiol*. 2007;293:C172–C83. doi:10.1152/ajpcell.00349.2006
59. Gao Z, Xu HG, Zhang XL, et al. [NF-kappaB signaling pathway regulate endplate chondrocytes in rat vitro natural degeneration model]. *Zhonghua Yi Xue Za Zhi*. 2016;96:2182–2186. doi:10.3760/cma.j.issn.0376-2491.2016.27.016
60. Deng W, Chen W, Clement S, et al. Controlled gene and drug release from a liposomal delivery platform triggered by X-ray radiation. *Nat Commun*. 2018;9:2713. doi:10.1038/s41467-018-05118-3
61. Wonder E, Simon-Gracia L, Scodeller P, et al. Competition of charge-mediated and specific binding by peptide-tagged cationic liposome-DNA nanoparticles in vitro and in vivo. *Biomaterials*. 2018;166:52–63. doi:10.1016/j.biomaterials.2018.02.052
62. Motomura M, Ichihara H, Matsumoto Y. Nano-chemotherapy using cationic liposome that strategically targets the cell membrane potential of pancreatic cancer cells with negative charge. *Bioorg Med Chem Lett*. 2018;28:1161–1165. doi:10.1016/j.bmcl.2018.03.013
63. Digiacomo L, Palchetti S, Pozzi D, Amici A, Caracciolo G, Marchini C. Cationic lipid/DNA complexes manufactured by microfluidics and bulk self-assembly exhibit different transfection behavior. *Biochem Biophys Res Commun*. 2018;503:508–512. doi:10.1016/j.bbrc.2018.05.016
64. Zhang X, Kong M, Tian MP, et al. The temperature-responsive hydroxybutyl chitosan hydrogels with polydopamine coating for cell sheet transplantation. *Int J Biol Macromol*. 2018;120:152–158. doi:10.1016/j.ijbiomac.2018.08.015
65. Chen Y, Zhang J, Li J, et al. Triptolide inhibits B7-H1 expression on proinflammatory factor activated renal tubular epithelial cells by decreasing NF-κB transcription. *Mol Immunol*. 2006;43:1088–1098. doi:10.1016/j.molimm.2005.07.026
66. Zhang S, Chuah SJ, Lai RC, Hui JHP, Lim SK, Toh WS. MSC exosomes mediate cartilage repair by enhancing proliferation, attenuating apoptosis and modulating immune reactivity. *Biomaterials*. 2018;156:16–27. doi:10.1016/j.biomaterials.2017.11.028
67. Yin H, Wang Y, Sun Z, et al. Induction of mesenchymal stem cell chondrogenic differentiation and functional cartilage microtissue formation for in vivo cartilage regeneration by cartilage extracellular matrix-derived particles. *Acta Biomater*. 2016;33:96–109. doi:10.1016/j.actbio.2016.01.024
68. Watanabe Y, Harada N, Sato K, Abe S, Yamanaka K, Matsushita T. Stem cell therapy: is there a future for reconstruction of large bone defects? *Injury*. 2016;47(Suppl 1):S47–S51. doi:10.1016/S0020-1383(16)30012-2
69. Kim C, Jeon OH, Kim DH, et al. Local delivery of a carbohydrate analog for reducing arthritic inflammation and rebuilding cartilage. *Biomaterials*. 2016;83:93–101. doi:10.1016/j.biomaterials.2015.12.029
70. Panjapheree K, Kamonmattayakul S, Meesane J. Biphasic scaffolds of silk fibroin film affixed to silk fibroin/chitosan sponge based on surgical design for cartilage defect in osteoarthritis. *Mater Design*. 2018;141:323–332. doi:10.1016/j.matdes.2018.01.006
71. Gandhi M, Bhatt P, Chauhan G, Gupta S, Misra A, Mashru R. IGF-II-conjugated nanocarrier for brain-targeted delivery of p11 gene for depression. *AAPS PharmSciTech*. 2019;20:50. doi:10.1208/s12249-018-1206-x
72. Bulbake U, Kommineni N, Ionov M, Bryszewska M, Khan W. Comparison of Cationic Liposome and PAMAM Dendrimer for Delivery of Anti-PIK1 siRNA in Breast Cancer Treatment. *Pharm Dev Technol*. 2019;1–27. doi:10.1080/10837450.2019.1567763
73. Behrendt P, Feldheim M, Preusse-Prange A, et al. Chondrogenic potential of IL-10 in mechanically injured cartilage and cellularized collagen ACI grafts. *Osteoarthritis Cartilage*. 2018;26:264–275. doi:10.1016/j.joca.2017.11.007
74. Rey-Rico A, Venkatesan JK, Schmitt G, Speicher-Mentges S, Madry H, Cucchiari M. Effective remodelling of human osteoarthritic cartilage by sox9 Gene transfer and overexpression upon delivery of rAAV vectors in polymeric micelles. *Mol Pharm*. 2018. doi:10.1021/acs.molpharmaceut.8b00331
75. Jiang M, Fu X, Yang H, Long F, Chen J. mTORC1 signaling promotes limb bud cell growth and chondrogenesis. *J Cell Biochem*. 2017;118:748–753. doi:10.1002/jcb.25728
76. Samuel S, Ahmad RE, Ramasamy TS, Karunanithi P, Naveen SV, Kamarul T. Platelet-rich concentrate in serum-free medium enhances cartilage-specific extracellular matrix synthesis and reduces chondrocyte hypertrophy of human mesenchymal stromal cells encapsulated in alginate. *Platelets*. 2019;30:66–74.
77. Hu D, Shan X. Effects of different concentrations of type-I collagen hydrogel on the growth and differentiation of chondrocytes. *Exp Ther Med*. 2017;14:5411–5416. doi:10.3892/etm.2017.5202
78. Hou C, Bai H, Wang Z, et al. A hyaluronan-based nanosystem enables combined anti-inflammation of mTOR gene silencing and pharmacotherapy. *Carbohydr Polym*. 2018;195:339–348. doi:10.1016/j.carbpol.2018.04.113
79. Digiacomo L, Palchetti S, Pozzi D, Amici A, Caracciolo G, Marchini C. Cationic lipid/DNA complexes manufactured by microfluidics and bulk self-assembly exhibit different transfection behavior. *Biochem Biophys Res Commun*. 2018. doi:10.1016/j.bbrc.2018.05.016
80. Lechanteur A, Sanna V, Duchemin A, Evrard B, Mottet D, Piel G. Cationic liposomes carrying siRNA: impact of lipid composition on physicochemical properties, cytotoxicity and endosomal escape. *Nanomaterials*. 2018;8. doi:10.3390/nano8050270

Supplementary material

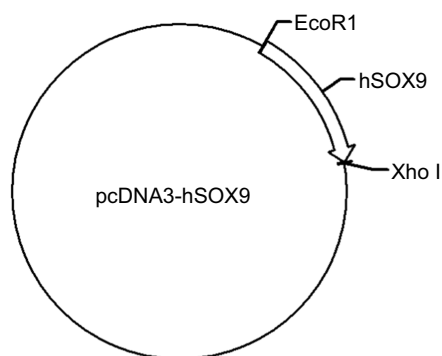


Figure S1 Homo sapiens (human) with vector backbone of pcDNA3

International Journal of Nanomedicine

Dovepress

Publish your work in this journal

The International Journal of Nanomedicine is an international, peer-reviewed journal focusing on the application of nanotechnology in diagnostics, therapeutics, and drug delivery systems throughout the biomedical field. This journal is indexed on PubMed Central, MedLine, CAS, SciSearch®, Current Contents®/Clinical Medicine,

Journal Citation Reports/Science Edition, EMBase, Scopus and the Elsevier Bibliographic databases. The manuscript management system is completely online and includes a very quick and fair peer-review system, which is all easy to use. Visit <http://www.dovepress.com/testimonials.php> to read real quotes from published authors.

Submit your manuscript here: <https://www.dovepress.com/international-journal-of-nanomedicine-journal>